International Journal of Thermophysics, Vol. 24, No. 6, November 2003 (© 2003)

PVTx and Isochoric Heat Capacity Measurements for Aqueous Methanol Solutions

M. M. Aliev,[1] J. W. Magee,[2] and I. M. Abdulagatov[1–3]

Received August 19, 2003

Isochoric heat capacity and *PVTx* properties of an aqueous methanol solution (0.50 mass fraction or 0.36 mole fraction of methanol) were measured in the liquid phase with a twin-cell adiabatic calorimeter. Temperatures ranged from 333 to 422 K, and pressures ranged to 20 MPa. The calorimetric cell (70 cm^3 capacity) was surrounded by adiabatic thermal shielding (high vacuum) and a steel-sheathed electric heater wound tightly on its surface. By combining the various sources of experimental uncertainty using a root-sum-of-squares formula, the relative uncertainty of C_V is estimated to be 2%. The uncertainties of the density, temperature (absolute), and pressure measurements are, respectively, about 0.1%, 40 mK, and ± 7 kPa. The measured densities were used to calculate excess molar volumes that were compared with values calculated with a reliable model by Simonson et al. Good agreement within $\pm 0.008\ cm^3 \cdot mol^{-1}$ (or $\pm 0.03\%$ of the density) was found between measured values of excess molar volume and those calculated from the model. Values of saturated liquid densities were determined by extrapolating experimental *P-T* data to the saturation curve.

KEY WORDS: aqueous solution; coexistence curve; critical point; density; excess molar volume; isochoric heat capacity; methanol; vapor pressure; water.

1. INTRODUCTION

Due to their high polarity, water and alcohol are complicated liquids and are a challenge to study both experimentally and theoretically. Their mixtures form a quite complex liquid system. If a small amount of alcohol is

[1] Institute for Geothermal Problems of the Dagestan Scientific Center of the Russian Academy of Sciences, Shamilya Str. 39-A, Makhachkala 367003, Dagestan, Russia.
[2] Physical and Chemical Properties Division, National Institute of Standards and Technology, 325 Broadway, Boulder, Colorado 80305, U.S.A.
[3] To whom correspondence should be addressed. E-mail: ilmutdin@boulder.nist.gov

0195-928X/03/1100-1551/0 © 2003 Plenum Publishing Corporation

added to water, the water structure becomes enhanced in a way similar to that found when a nonpolar solute is dissolved in water. Methanol is a small and highly polar molecule, and may be expected to interact strongly with other fluids in a hydrogen-bonded network [1]. In contrast to physical interactions, chemical interactions (hydrogen-bonding) are short-ranged and highly directional [2]. Chemical interactions by hydrogen-bonding can lead to the formation of new species, called either associated or solvated. Thermodynamic properties of polar fluids and fluid mixtures such as methanol and water + methanol are basically governed by chemical (hydrogen-bonding) interactions.

In mixtures in which methanol is one of the components, the thermodynamic properties may exhibit anomalies. Methanol molecules strongly affect, for example, water structure [3–6]; therefore, mixtures of methanol + water show anomalies in various physical properties. For example, the heat capacity shows a maximum at small concentrations of methanol (about 10 mol%) at fixed temperature and pressure. Sound absorption in water + methanol mixtures decreases with an increase in temperature [7, 8]. Sound speed has a maximum and adiabatic compressibility has a minimum in water + methanol mixtures [9]. The hydrophobic parts of methanol molecules are also responsible for the anomalies in some thermodynamic properties of $H_2O + CH_3OH$, and in particular, the minimum in the partial molar volume [10, 11], the heat-capacity anomaly, and some features of the structure of dilute aqueous methanol mixtures [12].

Thermodynamic properties ($PVTx$ and C_VVTx) of associated fluid mixtures such as water + methanol provide insight to our understanding of the effect of hydrogen-bonding on thermodynamic behavior. Heat capacity is a very sensitive tool for studying structural changes in fluids and fluid mixtures.

A knowledge of the $PVTx$ and C_VVTx properties of water + alcohol mixtures over a wide temperature and pressure range is of interest in understanding the role of hydrogen bonding and other non-electrostatic effects in solvation. These data will prove to be useful to develop a physicochemical model of the thermodynamic properties of hydrogen-bonding mixtures such as water + methanol. Methanol and its aqueous solutions are also of technological interest for various applications such as transport and storage of hydrogen, natural refrigerants, and working fluids in new power cycles.

2. LITERATURE REVIEW

The thermodynamic properties of $H_2O + CH_3OH$ mixtures have been reported by many authors. Table I shows the available thermodynamic

data sets for H_2O+CH_3OH mixtures. In this table the first author and the year published are given together with the method employed, the uncertainty indicated by the authors, and the temperature, pressure, and concentration ranges. It is apparent that experimental isochoric and isobaric heat capacity data for H_2O+CH_3OH mixtures are scarce. Most of the data cover very limited ranges of temperature, pressure, and concentration. Thus, the primary objective of this work was to expand the existing thermodynamic database. The available experimental critical curve data sets are given in Table II. A brief analysis of the different data sets is given below.

2.1. *PVTx* Measurements

The *PVTx* properties of H_2O+CH_3OH mixtures were measured by a variety of methods (see Table I). Most of them employed various types of densimeters. Most of the data were obtained after 1980. No data were available in the vapor phase (except Shahverdiyev and Safarov [16]) and in the critical region (except Bazaev et al. [38]). Most of the reported *PVTx* data cover a low temperature range (up to 420 K) and limited compositions in the liquid phase. Almost all reported density data were used to calculate excess molar volumes in the liquid phase. Data for the liquid phase at atmospheric pressure were reported by Dalager [25], Benson and Kiyohara [28], Patel and Sandler [29], McGlashan and Williamson [30], Friedman and Scheraga [33], Chen and Knapp [35], Mikhail and Kimel [39], and Clifford and Campbell [40]. The reported data agree well with one another.

Recently Yokoyama and Uematsu [13] measured *PVTx* properties of pure methanol and H_2O+CH_3OH mixtures in the high-density (between 652 and 1008 $kg \cdot m^{-3}$) liquid-phase region. Measurements of vapor pressure, bubble pressure, and saturated-liquid density are also reported. The bubble pressures reported by Yokoyama and Uematsu [13] agree well with the data by McGlashan and Williamson [30], Kurihara et al. [23], Griswold and Wong [29], and Bao et al. [24] within their mutual uncertainty.

Earlier Osada et al. [14] reported measurements of *PVTx*, vapor pressure, bubble pressure, and saturated-liquid density for this system. To compare with literature data, the bubble pressures were measured at two temperatures, 323.137 and 373.15 K. Good agreement was found with the data reported by McGlashan and Williamson [30], Kurihara et al. [23], and Bao et al. [24], while the data by Griswold and Wong [19] at a temperature of 373.15 K are lower than the data reported by Osada et al. [14]. They measured densities for a H_2O+CH_3OH mixture for the 0.5 mole

Table I. Summary of Thermodynamic Property Measurements for Aqueous Methanol Mixtures[a]

First author	Year	Method	Property	Uncertainty	Temperature (K)	Pressure (MPa)	Concentration (mole fraction)
Yokoyama [13]	2003	VV	$PVTx$, ρ'_s, P_s	0.002ρ	320–420	b.p.-200	0.2034 to 1.00
Osada [14]	1999	MBVV	$PVTx$, ρ'_s, P_s	0.001ρ	320–420	up to 200	0.49993 and 1.00
Xiao [15]	1997	VTD	$PVTx$, V_m^E	0.05 kg·m^{-3}	323–573	7–13.5	0 to 1
Shahverdiyev [16]	1992	CVP	$PVTx$, ρ'_s, P_s	0.03ρ (liq.) 0.09ρ (vap.)	298–523	b.p.–60	0.25 to 0.75
Kubota [17]	1987	MAP, HPB	$PVTx$,	0.05%	283–348	up to 350	0 to 1
Kubota [18]	1979	HPB	$PVTx$,	0.09%	283–348	up to 250	0 to 1
Griswold [19]	1952	PES	$Ptxy$ (VLE)	0.5% in P	373–523	up to 8.5	0.02 to 0.98
Schroder [20]	1959	CP	PTx (VLE)	0.001 m.f. 0.4% in P	413	up to 11	0.096 to 0.962
Kurihara [23]	1995	ES	PTx (VLE)	0.03 kPa	323–333	0.03–0.07	0.25, 0.50, 0.78
Bao [24]	1995	SA	PTx (VLE)	0.3%	353–403	0.064–0.815	0 to 1
Dalager [25]	1969	MES	VLE	n.a.	338–373	0.1	0 to 1
Easteal [26, 27]	1985	BV	$PVTx$, V_m^E	0.005 cm^3·mol^{-1}	278–323	up to 280	0 to 1
Benson [28]	1980	FTOTD	$PVTx$, V_m^E	0.02 kg·m^{-3}	288–308	0.1	0 to 1
Patel [29]	1985	VTD	V_m^E	0.05%	298.15	0.1	0.12 to 0.99
McGlashan [30]	1976	PM	$PVTx$, G_m	0.05 kg·m^{-3}	298.15, 308–338	0.1	0.041 to 1.0
Götze [31, 32]	1980	DM	V_m^E	0.003 cm^3·mol^{-1}	273–348	up to 250	0.5
Friedman [33]	1965	PM	$PVTx$, $\bar{V}_m^\infty$	10 ppm	274–323	0.1	0 to 0.011
Sentenac [34]	1998	VO	$PVTx$, P_S	0.2%	257–442, 363–442	up to 40	0.106 to 0.906
Chen [35]	1995	VTD	$PVTx$, V_m^E	0.05 kg·m^{-3}	283–313	0.1	0 to 1
Aliev [36]	1988	VVP	$PVTx$	0.063%	283–424	up to 140	0.1942 to 0.5675
Kuroki [37]	2001	TCTC	$PVTx$	0.2%	283–393	up to 21	0.2335 to 0.7055
Bazaev [38]	2003	CVP	$PVTx$	0.15%	373–673	0.042–91	0.36
Mikhail [39]	1961	PM	$PVTx$	0.05%	298–323	0.1	0 to 1
Clifford [40]	1951	PM	$PVTx$	0.04 kg·m^{-3}	298	0.1	0 to 1
Gibson [41]	1935		$PVTx$		298	100	0 to 1

Moriyoshi [42]	1977	CVP	$PVTx$, K_T	0.2%	298.15	101	0.017 to 0.123
Ref. [43]	1976	evaluated data	H_m^E, V_m^E G_m^E	50 J·mol^{-1}, 0.03 cm^3·mol^{-1}	273–373	0.1	0 to 1
Simonson [1]	1987	FTMC	H_m^E	3% or 30 J·mol^{-1}	298–573	7–40	0.02 to 0.94
Wormald [44]	2000	CCWCFC	H_m^E	1%	373–573	0.1 to 13	0.5
Wormald [45]	1996	DFC	H_m^E	1%	423–523	up to 20	0.5
Busey [46]	1984	HPFMC	H_m^E	n.a.	573	up to 40	0.5
Lama [47]	1965	BC	H_m^E	0.74%	298	0.1	0.029 to 0.935
Lentz [48]	177	C	H_m^E	1.40%	296	50 to 100	0 to 1
					296	200	0.15
Heintz [49]	1979	IFC	H_m^E	0.80%	298	up to 50	0.168 to 0.659
Benjamin [60]	1963	AC	H_m^E	0.20%	298	0.1	0.03 to 0.95
Duttachoudhury [61]	1974	TCS	H_m^E	n.a.	298, 313	0.1	0.04 to 0.87
Benson [50,51]	1980	FTMC	C_{Pm}	0.05 J·K^{-1}·mol^{-1}	288–308	0.1	0 to 1
	1982		C_{Pm}^E				
Kuroki [37]	2001	TCTC	$C_V VTx$	1%	283–393	up to 21	0.2335 to 0.7055
Polikhronidi [52]	2003	HTHPAC	$C_V VTx$, ρ_s', ρ_s''	2%	371–579	35	0.5
Abdulagatov [53]	2000	HTHPAC	$C_V VTx$, , ρ_s', ρ_s''	2–3%	435–645	45	0.36
Endo [8]	1992	Pulse	WPT	n.a.	278	0.1	0.304 to 0.835
Aliev [36]	1988	Pulse	WPT	0.06%	293–426	up to 147	0.1232 to 0.6922
This work	2003	TCTC	$PVTx$, $C_V VTx$	0.1%, 2%	333–422	up to 20	0.36

[a] VTD, vibrating tube densimeter; D, densimeter; PM, pycnometric method; DM, dilatometric methods; DD, digital densimeter (DMA 10); DW, densimeter (Weld type); HW, hydrostatic weighing method; VV, variable volumometer; VVP, variable volume piezometer; HPB, high-pressure burette; MAP, modified Adam's piezometer; PES, pressure equilibrium still; FTOTD, flow-type oscillating tube densimeter; SA, static apparatus; TCTC, twin-cell-type calorimeter; FTMC, flow-type microcalorimeter; CCWCFC, counter-current water-cooled flow calorimeter; IFC, isothermal flow calorimeter; DFC, differential flow calorimeter; BC, brass calorimeter; ES, equilibrium still (ebulliometer); VO, visual observation; MBVV, metal, bellows variable volumometer; CP, circulation apparatus; MES, modified equilibrium still; BV, bellows volumometer; AC, adiabatic calorimeter; TCS, twin calorimetric system; n.a., no uncertainty given in source reference; b.p., bubble point.

Table II. Summary of Critical Property Measurements for Aqueous Methanol Mixtures

First author	Property	Uncertainty in T_C measurements (K)	Uncertainty in P_C measurements (MPa)	Uncertainty in ρ_C measurements ($kg \cdot m^{-3}$)	Concentration range (mole fraction)
Marshall [56]	T_C	0.4	–	–	0.123–0.755
Polikhranidi [52]	T_C, ρ_C	0.2	–	1–2	0.500
Bazaev [38]	T_C, ρ_C, P_C	0.35	0.3	10	0.360
Xiao [15]	T_C, P_C	n.a.	n.a.	–	0.440
Griswold [19]	T_C, P_C	n.a.	n.a.	–	0.797

fraction composition at a temperature of 323.137 K. These data were compared with values measured by Kubota and Tsuda [18] and Xiao et al. [15]. The data by Kubota et al. [18] are larger (average differences of about 0.43%) than the data reported by Osada et al. [14]. The densities reported by Xiao et al. [15] are larger (differences of about 0.5%) than the data reported by Osada et al. [14] at a temperature of 323 K and at atmospheric pressure. The values of excess molar volume derived from density measurements by Osada et al. [14] at atmospheric pressure and at a temperature of 320 K are higher than the values reported in the literature by Kubota et al. [18], Götze et al. [31, 32], Easteal and Woolf [26], and Xiao et al. [15]. The difference is about 0.085 $cm^3 \cdot mol$.

Xiao et al. [15] measured the densities of $H_2O + CH_3OH$ mixtures relative to that of water in a vibrating-tube densimeter. Excess molar volumes V_m^E were calculated from the experimental densities for the mixtures by use of accurate equations of state (IAPWS [54] for water and IUPAC [55] for methanol).

Only one data set is available for the vapor phase at pressures up to 60 MPa (Shahverdiyev and Safarov [16]). They reported *PVTx* results for $H_2O + CH_3OH$ mixtures using a constant volume piezometer. The results of the measurements were used to develop a polynomial-type equation of state for the one-phase measurements and correlation equations for the bubble and coexistence curves. They also derived values of the cross second and third virial coefficients from density measurements in the vapor phase. The accuracy of the method was confirmed by *PVT* measurements for pure water.

Recently Bazaev et al. [38] reported *PVTx* relationships for the (0.64 mole fraction) H_2O + (0.36 mole fraction) CH_3OH mixture in the

near-critical and supercritical regions. Measurements were made with a constant-volume ($32.68 \pm 0.01\ cm^3$) piezometer surrounded by a precision thermostat. The values of the critical parameters (T_C, P_C, ρ_C) were extracted from the measured *PVTx* data (see Table II).

Easteal and Woolf [26, 27] measured *PVTx* data for H_2O + methanol mixtures for pure components and for six compositions and five temperatures between 278 and 323 K from which they derived excess molar volumes and excess molar enthalpy. These values of the excess molar volume were used to calculate other excess properties such as Gibbs energy, molar enthalpy, and molar entropy.

Götze et al. [31, 32] reported excess molar volumes for 0.5 H_2O + 0.5 CH_3OH. Measurements were made dilatometrically in a special stainless-steel mixing cell mounted in an autoclave. Differences between the data of Götze et al. [31, 32] and the data reported by McGlashan and Williamson [30], Gibson [41], and Clifford and Campbell [41] are within $0.013\ cm^3 \cdot mol^{-1}$.

2.2. Vapor-Liquid Equilibrium Measurements

Vapor-liquid equilibrium properties of $H_2O + CH_3OH$ mixtures have been reviewed and compiled extensively by Hirata et al. [22]. They reported a comprehensive review of all the $H_2O + CH_3OH$ measurements which were made between 1927 and 1975. Six selected VLE data sets for $H_2O + CH_3OH$ mixtures are given in Table I.

Bao et al. [24] used a static apparatus to measure VLE properties of $H_2O + CH_3OH$ mixtures. The results were correlated with Margules, NRTL, Van Laar, Wilson, and UNIQUAC liquid activity coefficient models. Griswold and Wong [19] measured the vapor-liquid phase equilibrium *PTxy* relationships (bubble and dew points) of $H_2O + CH_3OH$ mixtures at four isotherms of 373, 423, 473, and 523 K using the pressure equilibrium still. The values of the critical pressure and the critical temperature were determined from measured values of *PTx* (see Table II).

2.3. Heat Capacity Measurements

Only three data sets are available for the specific heat capacity at constant volume. All of these data were obtained between 2000 and 2003.

Kuroki et al. [31] reported isochoric heat capacities and densities for two $H_2O + CH_3OH$ mixtures (0.23351 and 0.70548 mole fractions) in the liquid phase. Measurements were made with a twin-cell type calorimeter.

Polikhronidi et al. [52] also measured the heat capacity at constant volume for (0.5 mole fraction) $H_2O + 0.5\ CH_3OH$ mixture. These data included the liquid-vapor coexistence curve, and critical and supercritical conditions. Measurements were made with a high-temperature, high-pressure, and nearly constant-volume calorimeter. The same apparatus was used previously to measure the isochoric heat capacity C_{VX} for (0.64 mole fraction) $H_2O + 0.36\ CH_3OH$ mixture by Abdulagatov et al. [53].

Benson et al. [50, 51] reported heat capacities at constant pressure of binary mixtures of water with methanol over the entire mole fraction range using a flow microcalorimeter. The obtained isobaric heat capacity data were used to calculate excess molar heat capacities. These data were included in the fits to a thermodynamically consistent empirical function of T, P, and x developed by Simonson et al. [1].

2.4. Other Thermodynamic Property Measurements

Other thermodynamic properties such as excess molar enthalpies, partial molar volumes, Gibbs free energies, sound speeds, compressibility, and saturation property data of $H_2O + CH_3OH$ mixtures reported in the literature are given in Table I. Most of the available measurements of excess enthalpy were made in the liquid phase only.

Simonson et al. [1] measured excess molar enthalpies of $H_2O + CH_3OH$ mixtures using a flow-type microcalorimeter. The results were combined with thermodynamic data reported by other authors to calculate excess molar Gibbs free energies, excess molar volumes, excess molar enthalpies, and excess molar heat capacities from fitting equations. They developed an equation with 32 adjustable parameters to fit the temperature, pressure, and composition dependence of G_m^E, H_m^E, V_m^E, and $C_{p,m}^E$ for $H_2O + CH_3OH$ mixtures over the range from 298 to 523 K and at pressures up to 42 MPa.

Wormald and Yerlett [44] reported molar enthalpy increments for a (0.5 mole fraction) $H_2O + 0.5\ CH_3OH$ mixture. Measurements were carried out with a counter-current water-cooled flow calorimeter. The dew and bubble points were extracted from measured values of molar enthalpy increments using a graphical extrapolation technique. The measurements cover the gaseous, two-phase, liquid, and supercritical regions.

Earlier Wormald et al. [45] also measured excess enthalpies for $0.5\ H_2O + 0.5\ CH_3OH$ mixtures using a new differential-flow calorimeter for operation at high temperatures and pressures. The excess enthalpy data at a pressure of 7 MPa and at temperatures of 423.2 and 473.2 K reported by these authors were compared with values reported by Simonson et al. [1].

At 423.2 K and 0.5 mole fraction, the data by Wormald et al. [45] differ from the values reported by Simonson et al. [1] by 0.02 $kJ \cdot mol^{-1}$, while at a temperature of 473.2 K both measurements are the same, 0.5 $kJ \cdot mol^{-1}$.

Lama and Lu [47] reported experimental excess enthalpies for $H_2O + CH_3OH$ mixtures by means of brass calorimeters of various sizes. The measured excess enthalpies for water + methanol mixtures cover the complete concentration range. The uncertainty of the measurements arising from possible evaporation was 0.24%, and the uncertainty resulting from heat exchange with the surroundings amounted to 0.5%. Other measurement uncertainties were negligible. These data are systematically less (≈ 20 $J \cdot mol^{-1}$) than the data reported by Benjamin and Benson [60].

The sound absorption in water + methanol mixtures was studied by Endo et al. [8] by means of the pulse method at a temperature of 278 K. The sound absorption in water + methanol mixtures decreases with an increase in temperature and exhibits a maximum as a function of the methanol concentration. Sound speed and adiabatic compressibility values for water + methanol mixtures exhibit a maximum and a minimum, respectively, as a function of the methanol concentration [9].

Only one data set is available for the speed of sound of $H_2O + CH_3OH$ mixtures. These data were reported by Aliev [36] using the pulse method. Most data for other thermodynamic properties of $H_2O + CH_3OH$ mixtures were derived at atmospheric pressure and low temperatures (up to 310 K).

2.5. Critical Property Measurements

Table II shows the available critical properties data sets for $H_2O + CH_3OH$ mixtures together with concentration range and their uncertainties. No critical densities for $H_2O + CH_3OH$ mixtures have been reported in the literature except for the values reported by Bazaev et al. [38] and Polikhronidi et al. [52].

Marshall and Jones [56] reported liquid-vapor critical temperature curve data for $H_2O + CH_3OH$ mixtures over the complete range of composition, namely, 0.123, 0.232, 0.360, 0.511, and 0.755 mole fraction of methanol. For the composition of the present study ($x = 0.36$ mole fraction of methanol), the measured value of the critical temperature by Marshall and Jones [56] is $T_C = 583.15$ K. Measurements were made with a visual method. In this method the measured value of the critical temperature is that at which the meniscus separating the liquid and vapor phases disappears at equal volumes of the two phases. The critical temperature was measured with an uncertainty of ± 0.4 K. The uncertainty in concentration is ± 0.5 mass%.

The critical-temperature and the critical-density values were extracted from measured values of saturated densities (in calorimetric measurements by the method of quasi-static thermograms) near the critical point by Polikhronidi et al. [52] for the equimolar composition ($x=0.5$ mole fraction of methanol, $T_C=561.8$ K and $\rho_C=281.0\ \mathrm{kg\cdot m^{-3}}$).

Bazaev et al. [38] estimated the critical parameters (T_C, P_C, ρ_C) of a H_2O+CH_3OH mixture ($x=0.36$ mole fraction of methanol) using $PVTx$ measurements near the critical point (by observation of both isochoric and isothermal break points). Derived results are ($x=0.36$ mole fraction of methanol, $T_C=583.5$ K, $P_C=15.0$ MPa, and $\rho_C=290.0\ \mathrm{kg\cdot m^{-3}}$).

Xiao et al. [15] reported the following values of the critical parameters for a H_2O+CH_3OH mixture ($x=0.44$ mole fraction of methanol, $T_C=573.6$ K, $P_C=13.7$ MPa). The values of the critical temperature ($T_C=523.15$ K) and the critical pressure ($P_C=8.51$ MPa) reported by Griswold and Wong [19] for a water+methanol mixture ($x=0.797$ mole fraction of methanol) are considerably lower than those of other authors.

The present paper reports the results of thermal (PVT) and caloric (C_VVT) properties measurements for a H_2O+CH_3OH mixture ($x=0.36$ mole fraction of methanol). Pressure versus temperature data were measured at constant density (quasi-isochores). Four quasi-isochores ranging in density from 812 to 879 $\mathrm{kg\cdot m^{-3}}$ were measured. The data cover the temperature range from 333 to 422 K at pressures up to 20 MPa.

3. EXPERIMENTAL

Details of the apparatus, procedures, and uncertainties of the measured quantities have been provided in previous papers [57–59]. High-purity samples of water and methanol were used to prepare the mixture. The water sample was twice-distilled and has a minimum purity of 0.9999 mass fraction and an insulating resistivity of 18 $\mathrm{M\Omega\cdot cm}$. For the methanol sample, the commercial supplier clamed a minimum liquid purity of 0.998 mass fraction with 0.001 mass fraction H_2O and 0.0005 mass fraction C_2H_5OH. Each component was degassed twice and was stored in a light-weight cylinder. The sample cylinders were accurately weighed with a 2×10^{-4} g uncertainty.

The mixture was prepared in the calorimeter cell by introducing each component through evacuated tubing. The remaining mass in each cylinder was weighed and then the composition of the sample in the cell was calculated from the masses charged to the cell. The final mixture composition uncertainty is 0.0001 mass fraction.

4. RESULTS AND DISCUSSION

4.1. Heat Capacity and Density Measurements

Measurements of C_{VX} of the aqueous methanol solution (0.36 mole fraction) were carried out at four quasi-isochores (812.36, 841.83, 868.26, and 878.59 $kg \cdot m^{-3}$) for temperatures between 333 and 422 K and at pressures up to 22 MPa. The experimental isochoric heat capacity ($C_{VX}VT$) and density (PVT) results are given in Table III and shown in Figs. 1 to 3.

Figure 1 shows the one-phase isochoric heat capacity as a function of temperature along measured quasi-isochores. For the quasi-isochore of 868.26 $kg \cdot m^{-3}$, the measurements were made in the one- and two-phase regions (see Fig. 2). The two-phase isochoric heat capacity C_{VX} rises to a maximum at the phase transition temperature $T_S = 349.05 \pm 0.5$ K, and then drops discontinuously to a value corresponding to the one-phase region (see Fig. 2). Figure 3 shows the P-T diagram (bubble point curve) of the 0.64 H_2O + 0.36 CH_3OH mixture together with values of vapor pressures for the pure components calculated with IAPWS [54] and IUPAC [55] fundamental equations of state. This figure also presents one-phase PVT results and experimental bubble pressure data reported by other authors from the literature.

By extrapolation of experimental P-T curves (isochores) to the corresponding saturation temperatures (calculated with the correlation equation reported by Shahverdiyev and Safarov [16]) for each quasi-isochore, we derived values of bubble pressures P_S. The results are presented in Tables IV and V together with values of bubble pressures and saturated densities reported by other authors. The estimated uncertainty in derived values of P_S for this 0.64 H_2O + 0.36 CH_3OH mixture is 1%, after including the uncertainty in T_S.

Figures 4 and 5 show the comparisons between derived values of the saturated properties (P_S and ρ_S) and values reported by other authors. Comparisons with other results are difficult because of temperature, pressure, and concentration differences between the measurements. To compare our saturation property results (P_S, T_S, ρ_S), some data from the literature were interpolated to our temperatures, pressures, and concentration using a linear interpolation technique. Therefore, in Figs. 4 and 5 we approximately compare the present derived P_S-T_S and T_S-ρ_S results with values derived from data reported by other authors. The present results and all of the other published data sets are reasonably consistent. Good agreement up to 0.36% is found between the present derived values of the bubble pressure and the values reported by Yokoyama and Uematsu [13] at high temperatures, while at low temperatures the differences reached 3.6%.

Table III. Experimental Densities and Isochoric Heat Capacities for 0.64 $H_2O + 0.36\ CH_3OH$ Mixture

T_1 (K)	P (MPa)	ρ ($kg \cdot m^{-3}$)	C_V ($kJ \cdot kg^{-1} \cdot K^{-1}$)
	$\rho = 878.59\ kg \cdot m^{-3}$ (Run-1)		
336	4.712	879.55	3.3091
337	5.910	879.37	3.3527
338	7.105	879.19	3.3408
339	8.302	879.00	3.3969
340	9.499	878.82	3.3911
341	10.710	878.64	3.3799
342	11.915	878.45	3.3959
343	13.125	878.27	3.3764
344	14.323	878.08	3.3910
345	15.539	877.90	3.3638
346	16.756	877.71	3.3828
347	17.967	877.53	3.3856
	$\rho = 878.59\ kg \cdot m^{-3}$ (Run-2)		
335	3.518	879.74	3.3410
336	4.712	879.55	3.4105
337	5.914	879.37	3.3664
338	7.105	879.19	3.3847
339	8.303	879.00	3.3821
340	9.501	878.82	3.4191
341	10.709	878.64	3.3755
342	11.913	878.45	3.3768
343	13.116	878.27	3.4029
344	14.325	878.08	3.3916
345	15.534	877.90	3.4135
346	16.757	877.71	3.3537
347	17.963	877.53	3.3761
	$\rho = 868.26\ kg \cdot m^{-3}$ (Run-1)		
354	1.537	868.37	3.5010
355	2.711	868.19	3.3742
356	3.897	868.01	3.4006
357	5.088	867.83	3.4381
358	6.285	867.65	3.4499
359	7.485	867.47	3.4095
360	8.685	867.29	3.4501
361	9.885	867.11	3.4096
362	11.092	866.92	3.4537
363	12.302	866.74	3.4116
364	13.508	866.56	3.4150
365	14.712	866.38	3.4572
366	15.936	866.20	3.4157
367	17.145	866.01	3.3829
368	18.359	865.83	3.4425

Table III. *(Continued)*

T_1 (K)	P (MPa)	ρ (kg·m^{-3})	C_V (kJ·kg^{-1}·K^{-1})
		$\rho = 868.26$ kg·m^{-3} (Run-2)	
333	0.087	869.52	3.8777
334	0.089	869.48	3.8677
335	0.091	869.44	3.8726
336	0.094	869.40	3.9196
337	0.098	869.36	3.8906
338	0.102	869.32	3.8905
339	0.106	869.28	3.8721
340	0.111	869.24	3.9167
341	0.115	869.20	3.9008
342	0.119	869.16	3.8895
343	0.123	869.12	3.9064
344	0.129	869.08	3.9186
345	0.135	869.04	3.9348
346	0.143	868.99	3.9057
347	0.155	868.95	3.8996
348	0.170	868.91	3.9607
349	0.191	868.87	3.9627
350	0.224	868.82	3.9296
351	0.281	868.76	3.8710
352	0.412	868.68	3.9091
		$\rho = 841.83$ kg·m^{-3}	
381	2.613	842.96	3.2688
382	3.774	842.79	3.3835
383	4.948	842.61	3.3939
384	6.126	842.44	3.3774
385	7.294	842.27	3.4308
386	8.476	842.09	3.4233
387	9.653	841.92	3.4176
388	10.844	841.75	3.3855
389	12.017	841.57	3.3811
390	13.197	841.40	3.4262
391	14.398	841.22	3.3782
392	15.579	841.05	3.3841
393	16.768	840.88	3.3428
394	17.951	840.70	3.3823
		$\rho = 812.36$ kg·m^{-3} (Run-1)	
410	5.395	813.13	3.3508
411	6.527	812.97	3.2648
412	7.651	812.80	3.3465
413	8.776	812.65	3.3251
414	9.898	812.48	3.4818
415	11.036	812.32	3.2092
416	12.169	812.16	3.3495
417	13.300	812.00	3.2995
418	14.432	811.83	3.2954
419	15.579	811.67	3.2454
420	16.711	811.51	3.3672

Table III. *(Continued)*

T_1 (K)	P (MPa)	ρ ($kg \cdot m^{-3}$)	C_V ($kJ \cdot kg^{-1} \cdot K^{-1}$)
	$\rho = 812.36\ kg \cdot m^{-3}$ (Run-2)		
408	3.158	813.45	3.3386
409	4.273	813.29	3.3765
410	5.394	813.13	3.4288
411	6.521	812.97	3.3718
412	7.639	812.81	3.4035
413	8.769	812.65	3.3511
414	9.897	812.48	3.3955
415	11.035	812.32	3.3263
416	12.165	812.16	3.2830
417	13.305	812.00	3.3273
418	14.433	811.83	3.3648
419	15.576	811.67	3.3071
420	16.709	811.50	3.3199
421	17.846	811.35	3.2991

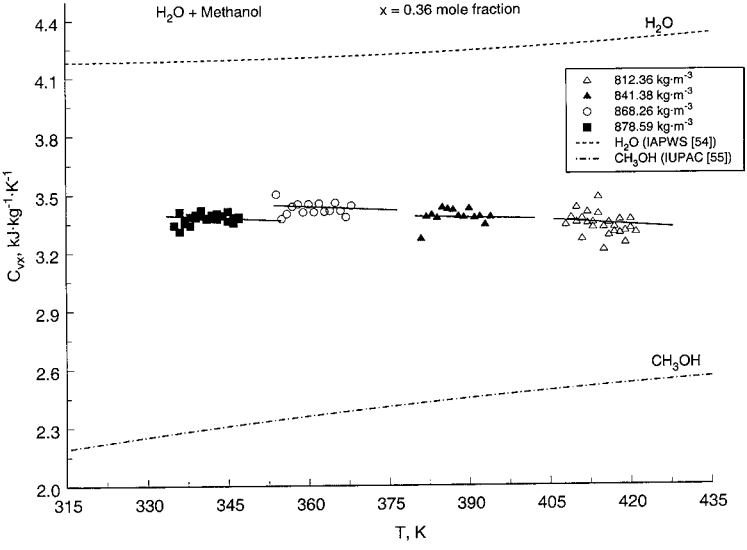

Fig. 1. Measured isochoric heat capacities C_{VX} as a function of temperature T along various quasi-isochores for a 0.64 H_2O + 0.36 CH_3OH mixture in the one-phase region.

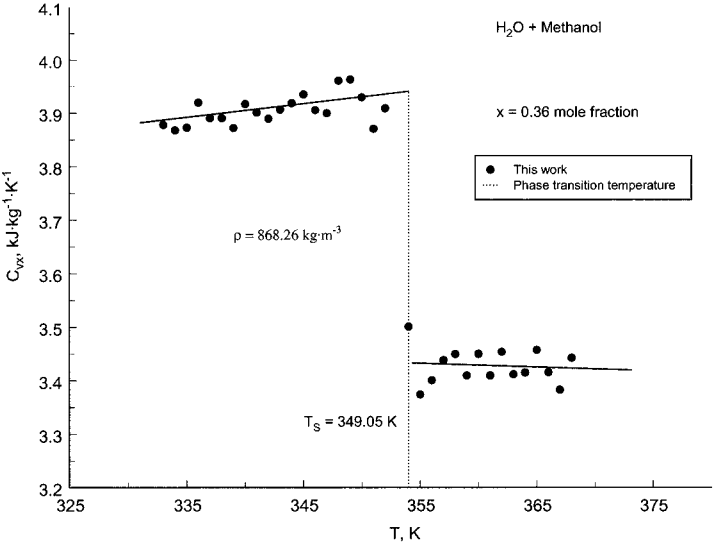

Fig. 2. Measured isochoric heat capacities C_{VX} as a function of temperature T along selected quasi-isochore 868.26 kg·m^{-3} for a H_2O+CH_3OH mixture in the one- and two-phase regions. Solid curve is a guide for the eye.

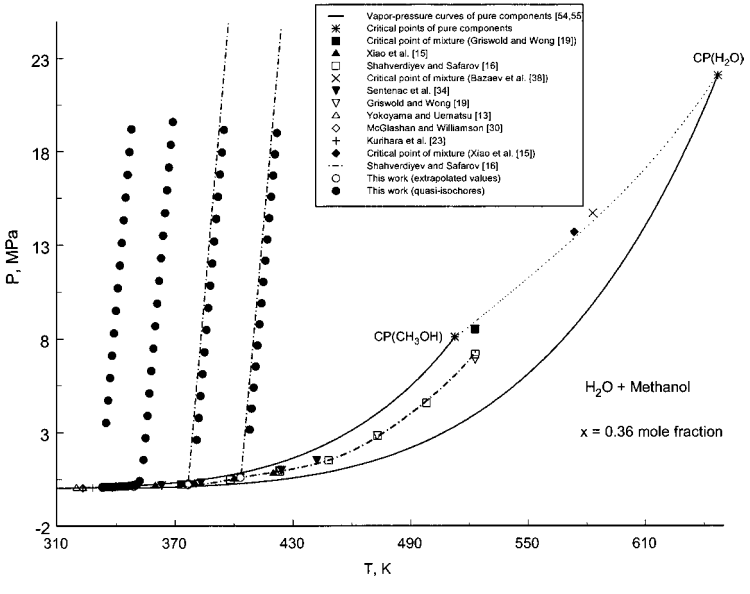

Fig. 3. $P-T$ diagram for 0.64 $H_2O+0.36$ CH_3OH mixture together with values for pure components. (⋯) critical curve (guide for the eye).

Table IV. Temperatures and Pressures at Saturation for H_2O+CH_3OH Mixture

T_S (K)	P_S (MPa) This work	P_S (MPa) [34]	P_S (MPa) [19]	P_S (MPa) [30]	P_S (MPa) [13]
			$x=0.36$ mole fraction		
403.26	0.5875	0.5941	0.6064	–	–
376.71	0.2725	0.2700	0.2749	–	0.2715
349.05	0.1099	–	–	–	0.1139
333.20	0.0559	–	–	0.0538	0.0600

Table V. Temperatures and Densities at Saturation for H_2O+CH_3OH Mixture

T_S (K)	ρ_S ($kg \cdot m^{-3}$) This work	ρ_S ($kg \cdot m^{-3}$) [13]
	$x=0.36$ mole fraction	
403.26	812.36	–
376.71	841.83	843.39
349.05	868.26	860.25
333.20	878.59	879.08

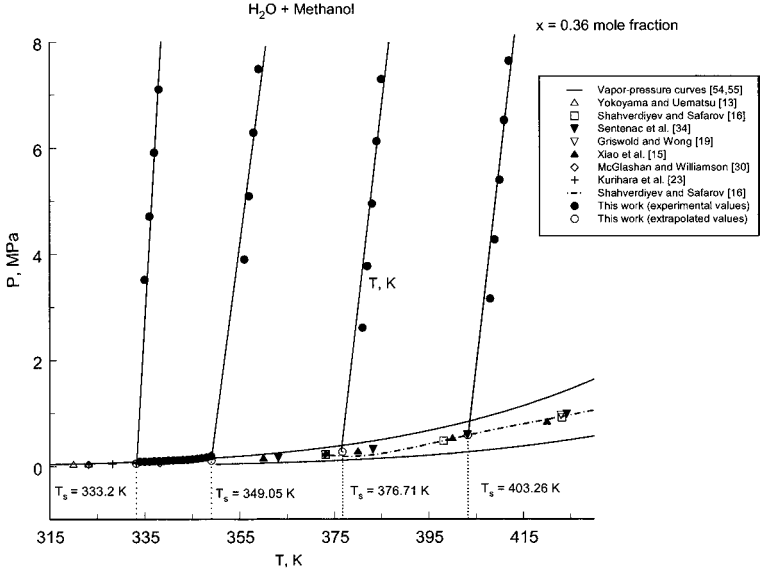

Fig. 4. Extrapolation of the measured P-T curves to vapor pressures at fixed isochores for 0.64 H_2O+0.36 CH_3OH mixture together with derived saturated temperatures T_S.

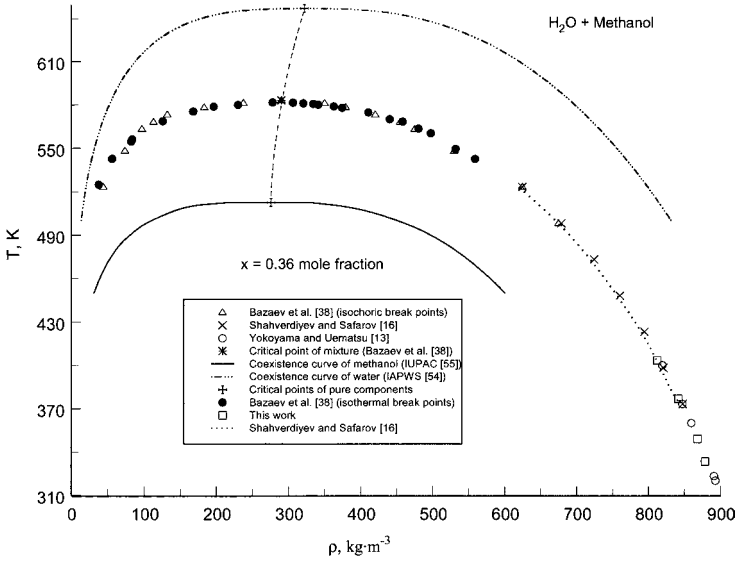

Fig. 5. Phase boundary in T–ρ-plane derived from present $PVTx$ measurements for the 0.64 H_2O+0.36 CH_3OH mixture together with values reported by other authors in the literature and values for pure components calculated with the IAPWS [54] and IUPAC [55] equations of state. (---) critical curve (guide for the eye).

Good agreement within 1.0% is observed also between the present results and the data reported by Sentenac et al. [34]. The data by Griswold and Wong [19] differ from the present results for bubble pressure by 0.88% at high temperatures and by up to 4.5% at low temperatures. The bubble pressure data reported by McGlashan and Williamson [30] deviate from the present values by 3%. Good agreement was found also for the derived saturation densities and the data reported by Yokoyama and Uematsu [13]. Deviations from the published data averaged 0.12% with a maximum deviation of 0.9%. The agreement is acceptable, because it is within the uncertainties introduced into the present saturation data due to the graphical and analytical extrapolation techniques.

Measured density data for 0.64 H_2O+0.36 CH_3OH were used to calculate excess molar volumes. Comparisons of the present results and the results by other authors with values calculated from the model by Simonson et al. [1] are given in Table VI and in Figs. 6a, 6b, 7a, and 7b. The average absolute deviation of experimental values at temperatures from 354 to 390 K and pressures between 2.7 and 13.2 MPa from the model was

Table VI. Comparisons of Experimental and Calculated Values of the Excess Molar Volume for Water + Methanol Mixtures

T (K)	P (MPa)	x (mole fraction)	V_m^E (calc.) ($cm^3 \cdot mol^{-1}$) Simonson et al. [1]	V_m^E(exp) ($cm^3 \cdot mol^{-1}$)	ΔV_m^E ($cm^3 \cdot mol^{-1}$)	δV_m^E (%)
			Xiao et al. [15]			
323.14	0.10	0.40888	−1.447	−1.021	0.426	−41.74
323.17	0.10	0.29674	−1.177	−0.876	0.301	−34.36
373.18	7.04	0.29674	−0.873	−0.873	0.000	0.03
373.19	7.01	0.40888	−1.017	−1.002	0.015	−1.46
373.20	13.49	0.40888	−0.945	−0.919	0.026	−2.88
373.19	13.49	0.29674	−0.814	−0.802	0.012	−1.47
423.38	7.00	0.29674	−1.079	−1.041	0.038	−3.66
423.29	7.00	0.40888	−1.281	−1.163	0.118	−10.13
423.21	13.53	0.40888	−1.020	−0.993	0.027	−2.70
423.19	13.53	0.29674	−0.879	−0.890	−0.011	1.29
			Osada et al. [14]			
400.00	10.0	0.50	−1.039	−0.925	0.11	−12.39
320.00	0.10	0.50	−1.298	−0.936	0.36	−38.66
			Kubota et al. [18]			
298.15	0.10	0.15	−0.472	−0.483	−0.011	2.33
323.15	0.10	0.15	−0.625	−0.529	0.096	−18.18
348.15	0.80	0.15	−0.568	−0.613	−0.046	7.45
298.15	0.10	0.25	−0.740	−0.746	−0.005	0.70
323.15	0.10	0.25	−1.020	−0.803	0.217	−27.06
348.15	3.50	0.25	−0.774	−0.835	−0.061	7.30
298.15	0.10	0.50	−1.010	−1.025	−0.016	1.52
323.15	0.10	0.50	−1.551	−1.078	0.472	−43.80
348.15	4.50	0.50	−1.029	−1.134	−0.105	9.27
298.15	0.10	0.75	−0.730	−0.730	0.000	0.02
323.15	0.10	0.75	−1.258	−0.784	0.474	−60.52
348.15	0.90	0.75	−0.937	−0.910	0.027	−2.95
			McGlashan and Williamson [30]			
298.15	0.10	0.15	−0.472	−0.490	−0.018	−3.80
298.15	0.10	0.25	−0.740	−0.745	−0.005	−0.67
298.15	0.10	0.75	−0.730	−0.723	0.007	0.97
			Götze and Shnieder [31]			
273.15	0.10	0.50	−0.399	−0.977	0.578	−59.16
298.15	0.10	0.50	−1.010	−0.988	−0.022	2.23
323.15	0.10	0.50	−1.551	−1.031	−0.520	50.44
273.15	10	0.50	−0.910	−0.894	−0.016	1.79
298.15	10	0.50	−0.941	−0.896	−0.045	5.02
323.15	10	0.50	−0.963	−0.920	−0.043	4.67
348.15	10	0.50	−0.977	−0.943	−0.034	3.61
273.15	50	0.50	−0.656	−0.650	−0.006	0.92

Table VI. *(Continued)*

T (K)	P (MPa)	x (mole fraction)	V_m^E (calc.) ($cm^3 \cdot mol^{-1}$) Simonson et al. [1]	V_m^E(exp) ($cm^3 \cdot mol^{-1}$)	ΔV_m^E ($cm^3 \cdot mol^{-1}$)	δV_m^E (%)
298.15	50	0.50	−0.663	−0.638	−0.025	3.92
323.15	50	0.50	−0.661	−0.635	−0.026	4.09
348.15	50	0.50	−0.651	−0.614	−0.037	6.03
			Shahverdiyev and Safarov [16]			
400	9.80	0.36	−0.983	−0.950	0.033	3.47
414	9.90	0.36	−1.026	−1.010	0.016	1.58
415	11.03	0.36	−1.002	−1.060	−0.058	−5.4
394	5	0.36	−1.103	−1.100	0.003	0.27
394	10	0.36	−0.967	−1.005	−0.038	−3.78
394	20	0.36	−0.856	−0.875	−0.019	−2.17
394	30	0.36	−0.765	−0.753	0.012	1.59
394	40	0.36	−0.678	−0.673	0.005	0.74
394	50	0.36	−0.593	−0.678	−0.085	−12.5
394	60	0.36	−0.508	−0.540	−0.032	−5.9
387	9.96	0.36	−0.955	−0.950	0.005	0.53
387	9.96	0.25	−0.760	−0.751	0.009	1.20
387	9.96	0.50	−1.011	−0.990	0.021	2.12
387	9.96	0.75	−0.700	−0.731	−0.031	−4.24
			Aliev [36]			
283.5	0.1	0.1942	−0.571	−0.621	−0.050	8.05
283.5	9.8	0.1942	−0.545	−0.576	−0.031	5.38
283.5	58.8	0.1942	−0.342	−0.383	−0.041	10.70
313.0	0.1	0.1942	−0.627	−0.638	−0.011	1.72
313.0	9.8	0.1942	−0.569	−0.586	−0.017	2.90
313.0	58.8	0.1942	−0.345	−0.406	−0.061	15.02
352.9	9.8	0.1942	−0.593	−0.620	−0.027	4.35
352.9	58.8	0.1942	−0.339	−0.428	−0.089	20.79
394.1	9.8	0.1942	−0.625	−0.740	−0.115	15.54
394.1	58.8	0.1942	−0.323	−0.446	−0.123	27.58
424.0	9.8	0.1942	−0.685	−0.851	−0.166	19.51
292.6	0.1	0.3599	−0.927	−0.942	−0.015	1.59
292.6	9.8	0.3599	−0.867	−0.875	−0.008	0.91
292.6	58.8	0.3599	−0.559	−0.600	−0.041	6.83
311.2	0.1	0.3599	−0.967	−0.969	−0.002	0.21
311.2	9.8	0.3599	−0.887	−0.886	0.001	−0.11
311.2	58.8	0.3599	−0.560	−0.576	−0.016	2.78
354.1	9.8	0.3599	−0.922	−0.886	0.036	−4.06
354.1	58.8	0.3599	−0.547	−0.531	0.016	−3.01
394.6	9.8	0.3599	−0.971	−0.954	0.017	−1.78
394.6	58.8	0.3599	−0.518	−0.496	0.022	−4.44
423.6	9.8	0.3599	−1.073	−1.029	0.044	−4.28

Table VI. *(Continued)*

T (K)	P (MPa)	x (mole fraction)	V_m^E (calc.) ($cm^3 \cdot mol^{-1}$) Simonson et al. [1]	V_m^E(exp) ($cm^3 \cdot mol^{-1}$)	ΔV_m^E ($cm^3 \cdot mol^{-1}$)	δV_m^E (%)
423.6	58.8	0.3599	−0.462	−0.469	−0.007	1.49
294.2	0.1	0.5675	−0.976	−1.025	−0.049	4.78
294.2	9.8	0.5675	−0.911	−0.954	−0.043	4.51
294.2	58.8	0.5675	−0.581	−0.667	−0.086	12.89
303.6	0.1	0.5675	−0.987	−1.001	−0.014	1.40
303.6	9.8	0.5675	−0.919	−0.926	−0.007	0.76
303.6	58.8	0.5675	−0.579	−0.641	−0.062	9.67
350.2	9.8	0.5675	−0.944	−0.881	0.063	−7.15
350.2	58.8	0.5675	−0.549	−0.577	−0.028	4.85
392.7	9.8	0.5675	−0.984	−0.935	0.049	−5.24
392.7	58.8	0.5675	−0.497	−0.631	−0.134	21.24
423.5	9.8	0.5675	−1.108	−1.042	0.066	−6.33
423.5	58.8	0.5675	−0.449	−0.597	−0.148	24.79
			Yokoyama and Uematsu [13]			
320	0.1	0.8005	−0.866	−0.581	0.285	−48.93
320	0.5	0.8005	−0.637	−0.584	0.052	−8.92
320	1.0	0.8005	−0.627	−0.589	0.038	−6.41
320	1.5	0.8005	−0.623	−0.588	0.036	−6.06
320	2.0	0.8005	−0.620	−0.576	0.044	−7.69
320	6.0	0.8005	−0.601	−0.549	0.052	−9.47
320	8.0	0.8005	−0.591	−0.527	0.064	−12.11
320	10.0	0.8005	−0.582	−0.536	0.046	−8.52
320	15.0	0.8005	−0.558	−0.497	0.061	−12.32
320	20.0	0.8005	−0.534	−0.455	0.079	−17.33
320	25.0	0.8005	−0.510	−0.449	0.061	−13.56
320	30.0	0.8005	−0.486	−0.426	0.060	−14.11
320	35.0	0.8005	−0.463	−0.411	0.052	−12.57
320	40.0	0.8005	−0.439	−0.385	0.053	−13.86
320	50.0	0.8005	−0.391	−0.356	0.035	−9.84
340	0.5	0.8005	−0.867	−0.585	0.281	−48.05
340	1.0	0.8005	−0.687	−0.597	0.090	−15.06
340	1.5	0.8005	−0.651	−0.608	0.043	−7.07
340	2.0	0.8005	−0.637	−0.606	0.031	−5.17
340	6.0	0.8005	−0.603	−0.568	0.035	−6.10
340	8.0	0.8005	−0.592	−0.554	0.038	−6.85
340	10.0	0.8005	−0.582	−0.536	0.046	−8.64
340	15.0	0.8005	−0.556	−0.511	0.045	−8.85
340	20.0	0.8005	−0.531	−0.453	0.078	−17.12
340	25.0	0.8005	−0.505	−0.440	0.065	−14.85
340	30.0	0.8005	−0.480	−0.437	0.043	−9.91
340	35.0	0.8005	−0.455	−0.412	0.042	−10.28
340	40.0	0.8005	−0.429	−0.397	0.033	−8.21
340	50.0	0.8005	−0.379	−0.360	0.018	−5.07

Table VI. *(Continued)*

T (K)	P (MPa)	x (mole fraction)	V_m^E (calc.) ($cm^3 \cdot mol^{-1}$) Simonson et al. [1]	V_m^E(exp) ($cm^3 \cdot mol^{-1}$)	ΔV_m^E ($cm^3 \cdot mol^{-1}$)	δV_m^E (%)
360	1.0	0.8005	−1.031	−0.645	0.387	−59.97
360	1.5	0.8005	−0.805	−0.636	0.169	−26.60
360	2.0	0.8005	−0.723	−0.625	0.099	−15.79
360	6.0	0.8005	−0.610	−0.590	0.020	−3.33
360	8.0	0.8005	−0.594	−0.581	0.013	−2.32
360	10.0	0.8005	−0.581	−0.545	0.036	−6.60
360	15.0	0.8005	−0.552	−0.540	0.011	−2.12
360	20.0	0.8005	−0.524	−0.479	0.045	−9.33
360	25.0	0.8005	−0.497	−0.453	0.044	−9.60
360	30.0	0.8005	−0.470	−0.441	0.028	−6.42
360	35.0	0.8005	−0.443	−0.422	0.021	−4.92
360	40.0	0.8005	−0.416	−0.405	0.010	−2.57
360	50.0	0.8005	−0.362	−0.360	0.002	−0.66
380	1.5	0.8005	−1.330	−0.701	0.629	−89.75
380	2.0	0.8005	−1.019	−0.678	0.341	−50.28
380	6.0	0.8005	−0.639	−0.628	0.011	−1.78
380	8.0	0.8005	−0.607	−0.596	0.011	−1.82
380	10.0	0.8005	−0.586	−0.562	0.024	−4.20
380	15.0	0.8005	−0.548	−0.548	−0.001	0.09
380	20.0	0.8005	−0.516	−0.499	0.016	−3.29
380	25.0	0.8005	−0.486	−0.453	0.033	−7.28
380	30.0	0.8005	−0.457	−0.444	0.013	−2.93
380	35.0	0.8005	−0.428	−0.430	−0.002	0.48
380	40.0	0.8005	−0.399	−0.373	0.026	−6.89
380	50.0	0.8005	−0.342	−0.346	−0.004	1.25
400	6.0	0.8005	−0.719	−0.662	0.057	−8.60
400	8.0	0.8005	−0.648	−0.648	0.000	0.00
400	10.0	0.8005	−0.608	−0.623	−0.014	2.31
400	15.0	0.8005	−0.550	−0.530	0.020	−3.73
400	20.0	0.8005	−0.510	−0.501	0.009	−1.84
400	25.0	0.8005	−0.475	−0.478	−0.003	0.63
400	30.0	0.8005	−0.443	−0.412	0.031	−7.45
400	35.0	0.8005	−0.411	−0.411	0.000	−0.07
400	40.0	0.8005	−0.380	−0.399	−0.019	4.88
400	50.0	0.8005	−0.319	−0.363	−0.044	12.23
320	1.0	0.4002	−0.999	−0.888	0.111	−12.53
320	1.5	0.4002	−0.994	−0.882	0.112	−12.74
320	2.0	0.4002	−0.990	−0.879	0.111	−12.64
320	6.0	0.4002	−0.961	−0.862	0.100	−11.58
320	8.0	0.4002	−0.947	−0.831	0.116	−13.91
320	10.0	0.4002	−0.933	−0.813	0.120	−14.72
320	15.0	0.4002	−0.897	−0.750	0.147	−19.61
320	20.0	0.4002	−0.861	−0.712	0.149	−21.00

Table VI. *(Continued)*

T (K)	P (MPa)	x (mole fraction)	V_m^E (calc.) ($cm^3 \cdot mol^{-1}$) Simonson et al. [1]	V_m^E(exp) ($cm^3 \cdot mol^{-1}$)	ΔV_m^E ($cm^3 \cdot mol^{-1}$)	δV_m^E (%)
320	25.0	0.4002	−0.825	−0.687	0.138	−20.11
320	30.0	0.4002	−0.789	−0.649	0.141	−21.66
320	35.0	0.4002	−0.754	−0.616	0.138	−22.43
320	40.0	0.4002	−0.718	−0.592	0.126	−21.19
320	50.0	0.4002	−0.646	−0.535	0.111	−20.75
360	1.0	0.4002	−1.409	−0.980	0.430	−43.86
360	1.5	0.4002	−1.198	−0.967	0.230	−23.81
360	2.0	0.4002	−1.120	−0.955	0.166	−17.36
360	6.0	0.4002	−1.002	−0.903	0.099	−10.95
360	8.0	0.4002	−0.981	−0.870	0.111	−12.82
360	10.0	0.4002	−0.963	−0.854	0.109	−12.76
360	15.0	0.4002	−0.920	−0.789	0.131	−16.62
360	20.0	0.4002	−0.879	−0.722	0.157	−21.76
360	25.0	0.4002	−0.838	−0.665	0.173	−26.08
360	30.0	0.4002	−0.797	−0.652	0.146	−22.37
360	35.0	0.4002	−0.757	−0.608	0.149	−24.48
360	40.0	0.4002	−0.717	−0.573	0.144	−25.13
360	50.0	0.4002	−0.636	−0.509	0.127	−24.91
400	6.0	0.4002	−1.139	−0.984	0.155	−15.78
400	8.0	0.4002	−1.064	−0.954	0.110	−11.58
400	10.0	0.4002	−1.019	−0.907	0.112	−12.40
400	15.0	0.4002	−0.946	−0.793	0.153	−19.27
400	20.0	0.4002	−0.891	−0.717	0.174	−24.29
400	25.0	0.4002	−0.841	−0.672	0.168	−25.05
400	30.0	0.4002	−0.793	−0.612	0.181	−29.61
400	35.0	0.4002	−0.746	−0.578	0.169	−29.19
400	40.0	0.4002	−0.700	−0.535	0.165	−30.89
400	50.0	0.4002	−0.609	−0.465	0.144	−30.89
320	1.0	0.2034	−0.641	−0.666	−0.025	3.71
320	1.5	0.2034	−0.638	−0.661	−0.023	3.50
320	2.0	0.2034	−0.635	−0.660	−0.025	3.75
320	6.0	0.2034	−0.616	−0.634	−0.019	2.92
320	8.0	0.2034	−0.606	−0.625	−0.019	3.01
320	10.0	0.2034	−0.597	−0.612	−0.016	2.60
320	15.0	0.2034	−0.572	−0.583	−0.010	1.80
320	20.0	0.2034	−0.548	−0.556	−0.008	1.45
320	25.0	0.2034	−0.524	−0.535	−0.011	2.06
320	30.0	0.2034	−0.500	−0.511	−0.011	2.18
320	35.0	0.2034	−0.476	−0.503	−0.027	5.42
320	40.0	0.2034	−0.452	−0.479	−0.027	5.73
320	50.0	0.2034	−0.403	−0.439	−0.035	8.04
360	1.0	0.2034	−0.846	−0.752	0.093	−12.39
360	1.5	0.2034	−0.746	−0.750	−0.004	0.59

Table VI. *(Continued)*

T (K)	P (MPa)	x (mole fraction)	V_m^E (calc.) ($cm^3 \cdot mol^{-1}$) Simonson et al. [1]	V_m^E(exp) ($cm^3 \cdot mol^{-1}$)	ΔV_m^E ($cm^3 \cdot mol^{-1}$)	δV_m^E (%)
360	2.0	0.2034	−0.708	−0.749	−0.040	5.39
360	6.0	0.2034	−0.646	−0.709	−0.063	8.85
360	8.0	0.2034	−0.633	−0.698	−0.065	9.37
360	10.0	0.2034	−0.621	−0.668	−0.047	7.09
360	15.0	0.2034	−0.592	−0.625	−0.033	5.22
360	20.0	0.2034	−0.564	−0.586	−0.021	3.63
360	25.0	0.2034	−0.537	−0.555	−0.018	3.21
360	30.0	0.2034	−0.510	−0.527	−0.018	3.38
360	35.0	0.2034	−0.482	−0.506	−0.024	4.67
360	40.0	0.2034	−0.455	−0.488	−0.033	6.71
360	50.0	0.2034	−0.401	−0.450	−0.050	11.03
400	6.0	0.2034	−0.723	−0.825	−0.103	12.43
400	8.0	0.2034	−0.683	−0.795	−0.113	14.15
400	10.0	0.2034	−0.657	−0.769	−0.112	14.56
400	15.0	0.2034	−0.613	−0.710	−0.097	13.71
400	20.0	0.2034	−0.577	−0.661	−0.084	12.69
400	25.0	0.2034	−0.544	−0.625	−0.081	12.91
400	30.0	0.2034	−0.512	−0.589	−0.076	12.94
400	35.0	0.2034	−0.481	−0.555	−0.074	13.28
400	40.0	0.2034	−0.450	−0.528	−0.077	14.68
400	50.0	0.2034	−0.389	−0.472	−0.083	17.60
			This work			
336	4.712	0.36	−0.947	−0.764	0.183	−23.95
337	5.910	0.36	−0.939	−0.751	0.188	−25.03
338	7.105	0.36	−0.930	−0.737	0.193	−26.19
339	8.302	0.36	−0.922	−0.724	0.198	−27.35
340	9.499	0.36	−0.914	−0.711	0.203	−28.55
341	10.710	0.36	−0.906	−0.697	0.209	−29.99
342	11.915	0.36	−0.898	−0.684	0.214	−31.29
343	13.125	0.36	−0.889	−0.672	0.217	−32.29
344	14.323	0.36	−0.881	−0.659	0.222	−33.69
345	15.539	0.36	−0.873	−0.647	0.226	−34.93
346	16.756	0.36	−0.864	−0.634	0.230	−36.28
347	17.967	0.36	−0.855	−0.625	0.230	−36.80
381	2.613	0.36	−1.208	−1.074	0.134	−12.48
382	3.774	0.36	−1.095	−1.053	0.042	−3.99
383	4.948	0.36	−1.044	−1.032	0.012	−1.16
384	6.126	0.36	−0.996	−1.012	−0.016	1.58
385	7.294	0.36	−0.992	−0.993	−0.001	0.10
386	8.476	0.36	−0.974	−0.973	0.001	−0.10
387	9.653	0.36	−0.959	−0.960	0.001	0.09
388	10.844	0.36	−0.946	−0.941	0.005	0.51
389	12.017	0.36	−0.933	−0.918	0.015	−1.63

Table VI. *(Continued)*

T (K)	P (MPa)	x (mole fraction)	V_m^E (calc.) ($cm^3 \cdot mol^{-1}$) Simonson et al. [1]	V_m^E(exp) ($cm^3 \cdot mol^{-1}$)	ΔV_m^E ($cm^3 \cdot mol^{-1}$)	δV_m^E (%)
390	13.197	0.36	−0.921	−0.900	0.021	−2.33
391	14.398	0.36	−0.909	−0.882	0.027	−3.06
392	15.579	0.36	−0.898	−0.866	0.032	−3.70
393	16.768	0.36	−0.887	−0.849	0.038	−4.48
394	17.951	0.36	−0.876	−0.835	0.041	−4.91
410	5.395	0.36	−1.211	−1.102	0.109	−9.89
411	6.527	0.36	−1.138	−1.075	0.063	−5.86
412	7.651	0.36	−1.090	−1.049	0.041	−3.91
413	8.776	0.36	−1.054	−1.025	0.029	−2.83
414	9.898	0.36	−1.026	−1.001	0.025	−2.50
415	11.036	0.36	−1.002	−0.977	0.025	−2.56
416	12.169	0.36	−0.982	−0.954	0.028	−2.94
417	13.300	0.36	−0.964	−0.932	0.032	−3.43
418	14.432	0.36	−0.948	−0.910	0.038	−4.18
419	15.579	0.36	−0.932	−0.888	0.044	−4.95
420	16.711	0.36	−0.917	−0.868	0.049	−5.65
410	5.394	0.36	−1.211	−1.102	0.109	−9.89
411	6.521	0.36	−1.138	−1.075	0.063	−5.86
412	7.639	0.36	−1.090	−1.050	0.040	−3.81
413	8.769	0.36	−1.054	−1.025	0.029	−2.83
414	9.897	0.36	−1.026	−1.001	0.025	−2.50
415	11.035	0.36	−1.002	−0.977	0.025	−2.56
416	12.165	0.36	−0.982	−0.954	0.028	−2.94
417	13.305	0.36	−0.964	−0.931	0.033	−3.54
418	14.433	0.36	−0.948	−0.910	0.038	−4.18
419	15.576	0.36	−0.932	−0.888	0.044	−4.95
420	16.709	0.36	−0.917	−0.868	0.049	−5.65
421	17.846	0.36	−0.903	−0.850	0.053	−6.24
354	1.537	0.36	−1.072	−1.026	0.046	−4.48
355	2.711	0.36	−1.007	−1.010	−0.003	0.30
356	3.897	0.36	−0.984	−0.994	−0.010	1.01
357	5.088	0.36	−0.969	−0.977	−0.008	0.82
358	6.285	0.36	−0.957	−0.961	−0.004	0.42
359	7.485	0.36	−0.947	−0.945	0.002	−0.21
360	8.685	0.36	−0.937	−0.930	0.007	−0.75
361	9.885	0.36	−0.927	−0.915	0.012	−1.31
362	11.092	0.36	−0.917	−0.899	0.018	−2.00
363	12.302	0.36	−0.908	−0.885	0.023	−2.60
364	13.508	0.36	−0.900	−0.870	0.030	−3.45
365	14.712	0.36	−0.889	−0.856	0.033	−3.86
366	15.936	0.36	−0.880	−0.842	0.038	−4.51
367	17.145	0.36	−0.870	−0.828	0.042	−5.07
368	18.359	0.36	−0.861	−0.814	0.047	−5.77

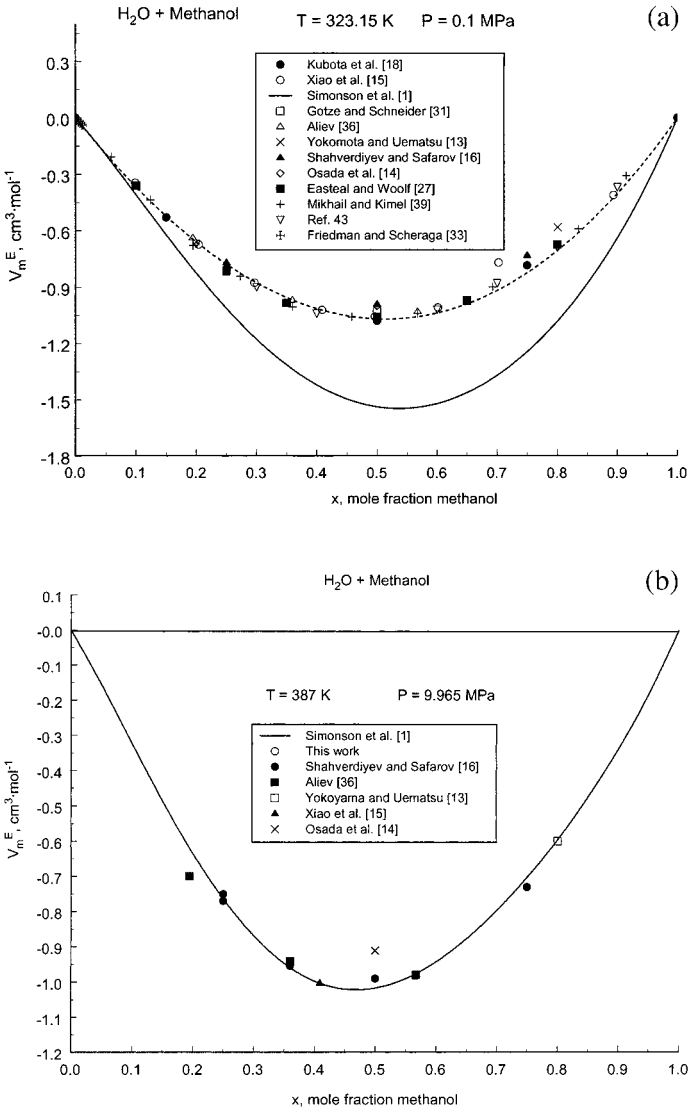

Fig. 6. Comparison between the excess molar volumes calculated with the model of Simonson et al. [1] and data reported by various authors in the literature for two selected temperatures and pressures: (a) 323.15 K and 0.1 MPa, (b) 387 K and 9.965 MPa. The dashed curve is a guide for the eye.

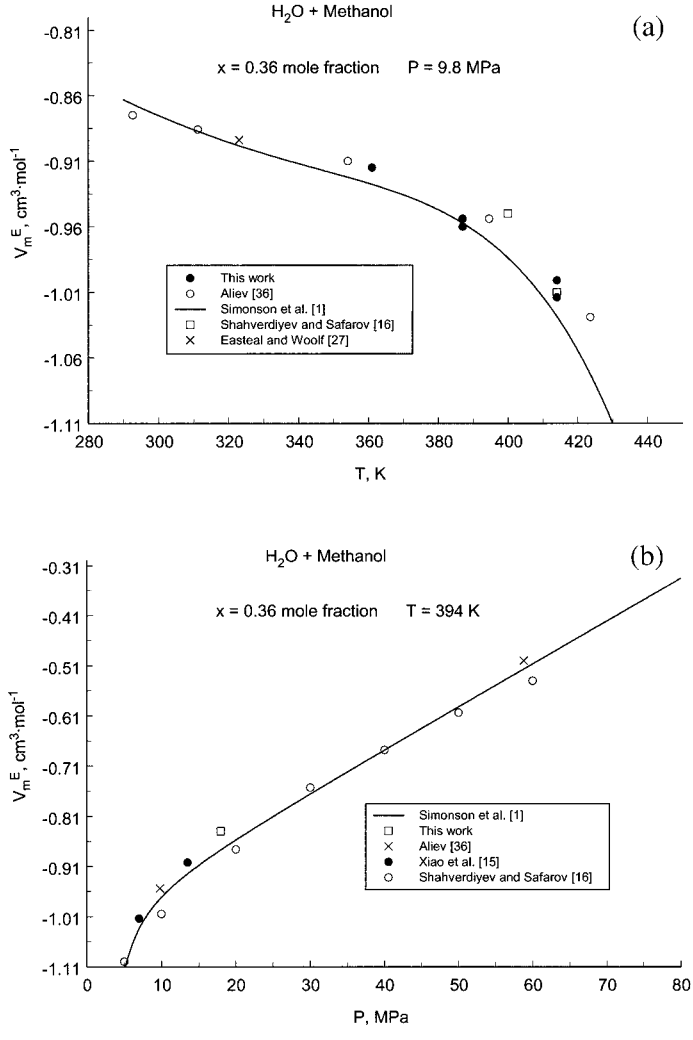

Fig. 7. Comparison of the (a) temperature and (b) pressure dependences of the excess molar volumes calculated with Simonson et al. [1] model and reported data.

determined to be $0.009\,cm^3 \cdot mol^{-1}$, which corresponds to a relative difference of 0.04% of the density. At temperatures below 350 K, the deviation is about 30%, while at high temperatures (above 390 K) the deviation is about ± 3 to 4%. As one can see from Figs. 6a and 6b, the agreement between various data sets is good (the scatter in all of the data are

about $\pm 1\%$) while the values of V_m^E calculated with the model of Simonson et al. [1] is systematically lower. At a concentration of 0.5 mole fraction, the deviation between reported data sets and calculated values of V_m^E is about 40% (corresponds to 1.5% difference in mixture molar volume). Good agreement within $\pm 1.3\%$ is observed between reported data and calculated values of V_m^E at 387 K and at a pressure of 9.97 MPa (see Fig. 6b). Figures 7a and 7b show good agreement (average deviation of about 2.5%) between published data sets and the model. At high temperatures ($T > 330$ K) and constant pressures ($P \approx 10$ MPa) the calculated values of excess molar volume are systematically lower (about 2 to 3%) than the reported data (see Fig. 7a). Good agreement is found between reported excess molar volume data and calculated values along the isotherm of 394 K (see Fig. 7b). Some data points in Figs. 6a, 6b, 7a, and 7b from the literature were analytically and graphically interpolated (linear interpolation technique) to the given temperatures, pressures, and concentrations due to differences between the measurements. The uncertainty of the interpolations is small (within their experimental uncertainty) especially in the range where the temperature, pressure, and concentration dependence of V_m^E is almost linear. To compare, we selected the values of V_m^E for the very close experimental temperatures, pressures, and concentrations.

5. CONCLUSIONS

By means of a twin-bomb calorimeter, isochoric heat capacities and densities of a liquid mixture 0.64 $H_2O + 0.36$ CH_3OH were measured in a range of temperature from 333 to 422 K, for densities between 812 and 879 $kg \cdot m^{-3}$, and pressures up to 20 MPa with respective estimated uncertainties of 2% and 0.1%. The measured densities were used to calculate excess molar volumes that were compared with values calculated from a model by Simonson et al. [1]. Good agreement within 0.0077 $cm^3 \cdot mol^{-1}$ (or 0.03% of the density) was found between the model and our measurements at temperatures from 355 to 385 K and pressures up to 11 MPa, while at temperatures from 411 to 420 and pressures up to 18 MPa the deviations reached to 0.03 $cm^3 \cdot mol^{-1}$ (or 0.15% of the density). The values of bubble pressures and densities at saturation were determined by extrapolating experimental *P-T* data to the saturated temperature.

ACKNOWLEDGMENT

I. M. Abdulagatov thanks the Physical and Chemical Properties Division at the National Institute of Standards and Technology for the

opportunity to work as a Guest Researcher at NIST during the course of this research. M. M. Aliev was supported by an IAPWS International Collaboration Project Award.

REFERENCES

1. J. M. Simonson, D. J. Bradley, and R. H. Busey, *J. Chem. Thermodyn.* **19**:479 (1987).
2. N. Asprion, H. Hasse, and G. Maurer, *Fluid Phase Equilib.* **205**:195 (2003).
3. Y. Marcus, *Phys. Chem. Chem. Phys.* **1**:2975 (1999).
4. A. Staib, *J. Chem. Phys.* **108**:4554 (1998).
5. G. Kabisch and K. Pollmer, *J. Mol. Struct.* **81**:35 (1982).
6. A. Laaksonen, P. G. Kusalik, and I. M. Svishchev, *J. Phys. Chem. A* **101**:5910 (1997).
7. W. D. T. Dale, P. A. Flavell, and P. Kurrus, *Can. J. Chem.* **54**:355 (1976).
8. H. Endo, K. Saijou, and G. Atkinson, *J. Acoust. Soc. Jpn.* **13**:85 (1992).
9. I. Larionov, Ph.D. thesis (MPPI, Moscow, 1951).
10. F. Franks, in *Water–A Comprehensive Treatise*, F. Franks, ed. (Plenum, New York, 1972), Vol. 2, Chap. 5.
11. B. Kvamme, *Phys. Chem. Chem. Phys.* **4**:942 (2002).
12. S. Yu. Noskov, M. G. Kiselev, and A. M. Kolker, *Russ. J. Structural Chem.* **40**:40 (1999).
13. H. Yokoyama and M. Uematsu, *J. Chem. Thermodyn.* **35**:813 (2003).
14. O. Osada, M. Sato, and M. Uematsu, *J. Chem. Thermodyn.* **31**:451 (1999).
15. C. Xiao, H. Bianchi, and P. R. Tremaine, *J. Chem. Thermodyn.* **29**:261 (1997).
16. A. N. Shahverdiyev and J. T. Safarov, *Phys. Chem. Chem. Phys.* **4**:979 (2002).
17. H. Kubota, Y. Tanaka, and T. Makita, *Int. J. Thermophys.* **8**:47 (1987).
18. H. Kubota, S. Tsuda, M. Murata, T. Yamamoto, Y. Tanaka, and T. Makita, *Rev. Phys. Chem. Jap.* **49**:59 (1979).
19. J. Griswold and S. Y. Wong, *Chem. Eng. Prog. Symp. Ser.* **48**:18 (1952).
20. W. Schroder, *Chem.-Ing.-Tech.* **30**:523 (1959).
21. M. Hirata and S. Suda, *Kagaku Kogaku* **31**:339 (1967).
22. M. Hirata, S. Ohe, and K. Nagahama, *Computer Aided Data of VLE* (Elsevier, Amsterdam, 1975).
23. K. Kurihara, T. Minoura, K. Takeda, and K. Kojima, *J. Chem. Eng. Data* **40**:679 (1995).
24. Z. Bao, M. Liu, J. Yang, and N. Wang, *J. Chem. Ind. Eng. (China)* **46**:230 (1995).
25. P. Dalager, *J. Chem. Eng. Data* **14**:298 (1969).
26. A. J. Easteal and L. A. Woolf, *J. Chem. Thermodyn.* **17**:49 (1985).
27. A. J. Easteal and L. A. Woolf, *J. Chem. Thermodyn.* **17**:69 (1985).
28. G. C. Benson and O. Kiyohara, *J. Sol. Chem.* **9**:791 (1980).
29. N. C. Patel and S. L. Sandler, *J. Chem. Eng. Data* **30**:218 (1985).
30. M. L. McGlashan and A. G. Williamson, *J. Chem. Eng. Data* **21**:196 (1976).
31. G. Götze and G. M. Schneider, *J. Chem. Thermodyn.* **12**:661 (1980).
32. G. Götze and P. Jeschke, *Ber. Buns.–Ges. Phys. Chem.* **81**:933 (1977).
33. M. E. Friedman and H. A. Scheraga, *J. Phys. Chem.* **69**:3795 (1965).
34. P. Sentenac, Y. Bur, E. Rauzy, and C. Berro, *J. Chem. Eng. Data* **43**:592 (1998).
35. G. Chen and H. Knapp, *J. Chem. Eng. Data* **40**:1001 (1995).
36. A. A. Aliev, Ph.D. thesis (Institute of Physics of the Azerbadjan Academy of Sciences, Baku, 1988).
37. T. Kuroki, N. Kagawa, H. Endo, S. Tsuruno, and J. W. Magee, *J. Chem. Eng. Data* **46**:1101 (2001).

38. A. R. Bazaev, I. M. Abdulagatov. J. W. Magee, E. A. Bazaev, and A. E. Ramazanova, to be submitted to *Int. J. Thermophys.*
39. S. Z. Mikhail and S. Z. Kimel, *J. Chem. Eng. Data* **6**:533 (1961).
40. G. Clifford and J. A. Campbell, *J. Am. Chem. Soc.* **73**:5449 (1951).
41. R. E. Gibson, *J. Am. Chem. Soc.* **57**: 1551 (1935).
42. T. Moriyoshi, Y. Morishita, and H. Inubushi, *J. Chem. Thermodyn.* **9**:577 (1977).
43. *Chem. Techn.* **28**:350 (1976).
44. C. J. Wormald and T. K. Yerlett, *J. Chem. Thermodyn.* **32**:97 (2000).
45. C. J. Wormald, L. Badock, and M. Lloyd, *J. Chem. Thermodyn.* **28**:603 (1996).
46. R. H. Busey, H. F. Holmes, and R. E. Mesmer, *J. Chem. Thermodyn.* **16**:343 (1984).
47. R. F. Lama and B. C.-Y. Lu, *J. Chem. Eng. Data* **10**:216 (1965).
48. H. Lentz, *Ber. Bunsenges. Phys. Chem.* **81**:1073 (1977).
49. A. Heintz and R. N. Lichtenthaler, *Ber. Bunsenges. Phys. Chem.* **83**:853 (1979).
50. G. C. Benson, P. J. D'Arcy, and O. Kiyohara, *J. Sol. Chem.* **9**:931 (1980).
51. G. C. Benson and P. J. D'Arcy, *J. Chem. Eng. Data* **27**:439 (1982).
52. N. G. Polikhronidi, I. M. Abdulagatov, J. W. Magee, and G. V. Stepanov, to be submitted to *Int. J. Thermophys.*
53. I. M. Abdulagatov, V. I. Dvoryanchikov, M. M. Aliev, and A. N. Kamalov, in *Steam, Water, and Hydrothermal Systems*, Proc. 13th Int. Conf. on the Properties of Water and Steam, P. R. Tremaine, P. G. Hill, D. E. Irish, and P. V. Balakrishnan, eds. (NRC Research Press, Ottawa, 2000), pp. 157–164.
54. W. Wagner and A. Pruß, *J. Phys. Chem. Ref. Data* **31**:387 (2002).
55. K. M. de Reuck and R. J. B. Craven, *International Thermodynamic Tables of the Fluid State-12. Methanol* (Blackwell Scientific, London, 1993).
56. W. L. Marshall and E. V. Jones, *J. Inorg. Nucl. Chem.* **36**:2319 (1974).
57. J. W. Magee, *Proc. 9th Symp. Energy Eng. Sci.*, Argonne National Laboratory (NTIS, Springfield, Virginia, 1991), pp. 318–322.
58. J. W. Magee, R. J. Deal, and J. C. Blanco, *J. Res. Natl. Inst. Stand. Technol.* **103**:63 (1998).
59. M. M. Aliev, J. W. Magee, and I. M. Abdulagatov, submitted to *Int. J. Thermophys.*
60. L. Benjamin and G. C. Benson, *J. Phys. Chem.* **67**:858 (1963).
61. M. K. Duttachoudhury and H. B. Mathur, *J. Chem. Eng. Data* **19**:145 (1974).